

Reduction of Threading Dislocations in GaN Overgrowth by MOCVD on TiN Porous Network Templates

F. Yun^{**1}, Y. Fu¹, Y. T. Moon¹, Ü. Özgür¹, J. Q. Xie¹, S. Doğan^{††1}, H. Morkoç¹, C. K. Inoki², T. S. Kuan², L. Zhou³, and D. J. Smith³

¹ Virginia Commonwealth University, Department of Electrical and Computer Engineering, Richmond, VA 23284

² Department of Physics, University at Albany, SUNY, Albany, NY 12222

³ Center for Solid State Science, Arizona State University, Tempe, AZ 85287

Received zzz, revised zzz, accepted zzz

Published online zzz

PACS 81.15.Gh, 68.37.Lp, 78.30.Fs

GaN overlayers for the purpose of reducing extended defects have been grown by MOCVD on porous network of TiN thin layers which in turn were achieved by *in situ* nitridation of thin Ti layers (20 nm and 10nm) on a GaN template. TEM analyses performed for the GaN layer with 20 nm TiN porous network indicate the effectiveness of TiN porous structure in blocking the threading dislocation from penetrating into the upper layer. Plane-view TEM indicated a reduction in the dislocation density by a factor of 10, compared to the GaN template without TiN network. Subsurface voids were formed during the TiN formation, which act as defect concentrators, and termination sites for dislocations. The reduction in defect density through the use of TiN porous networks is also confirmed by X-ray diffraction data and time-resolved photoluminescence measurements at room temperature.

© 2004 WILEY-VCH Verlag GmbH & Co. KGaA, Weinheim

1 Introduction GaN and related compounds have successfully penetrated the market place in terms of light emitting devices, and to a lesser extent light detecting devices. However, the impetus for improved devices as well as bringing high performance electronic devices to the market place is continually driving the GaN technology for improved optical and electrical properties which are severely affected by non-native substrates on which GaN is heteroepitaxially grown [1]. As such, heteroepitaxial GaN has a high density of threading dislocations (TDs) and associated point defects, which either scatter carriers, hamper radiative recombination efficiency or introduce instabilities, and they are detrimental to the operational lifetime and performance of devices [2]. In response to the TD problem, the epitaxial lateral overgrowth (ELO) technique has been developed and widely used to obtain device-quality GaN epilayers [3]. But, the ELO process requires *ex situ* photolithographic step(s), the frequency of which depends on how many times the process is repeated in a given structure, which is cumbersome at the very least and increases the cost. To circumvent this drawback, several groups have reported the micro-ELO method using *in situ* grown discontinuous SiN_x layer as mask [4,5]. This SiN_x layer is typically deposited on the GaN buffer layer by simultaneously introducing silane and ammonia gases into the MOCVD reactor. Improvements of the GaN quality grown on this *in situ* SiN_x layer have been achieved due to enhanced lateral overgrowth.

Oshima *et al* [6] has recently reported the growth of thick GaN and subsequent separation from sapphire substrate by a void-assisted separation (VAS) technique, which utilizes a thin TiN porous net-

** ** Corresponding author. Fax: +1-804-828-4269. E-mail address: fyun@vcu.edu.

†† Also with Atatürk University, Faculty of Art & Science, Department of Physics, 25240 Erzurum, Turkey.

© 2004 WILEY-VCH Verlag GmbH & Co. KGaA, Weinheim

work at the beginning of hydride vapor phase epitaxy (HVPE) growth. They obtained a very low TD density of $5 \times 10^6 \text{ cm}^{-2}$ for the 300- μm GaN layer on the TiN interlayer, as was reported by HVPE growth earlier in such GaN templates without a TiN network [7]. It is, therefore, interesting to determine the role of a TiN network on dislocation reduction in thinner GaN films. In this paper, we report the growth and characterization of GaN grown on *in situ* TiN porous network by MOCVD with reduced dislocation density and therefore improved optical and crystalline properties.

Sample#	Control	T68	CVD43
TiN layer	--	20 nm	10 nm
GaN overgrowth thickness (μm)	5.2 μm	7.5 μm	7.5 μm
XRD (002) FWHM (arcmin.)	3.9	3.8	5.0
XRD (102) FWHM (arcmin.)	7.6	5.4	4.5
Time-resolved PL Data (At room temperature)	$\tau_1=0.302 \pm 0.004 \text{ ns}$ $\tau_2=0.701 \pm 0.012 \text{ ns}$ $A_2/A_1=0.429$	$\tau_1=0.304 \pm 0.004 \text{ ns}$ $\tau_2=0.740 \pm 0.010 \text{ ns}$ $A_2/A_1=0.529$	$\tau_1=0.242 \pm 0.004 \text{ ns}$ $\tau_2=1.211 \pm 0.014 \text{ ns}$ $A_2/A_1=0.562$

Table I. List of GaN layers grown on 20 nm and 10 nm TiN porous networks, as well as the control GaN layer without TiN. The XRD data and time-resolved PL data are summarized here.

2 Experimental On the layer growth front, a 0.7 μm GaN grown on sapphire by MOCVD was used as templates. Ti films of 20 nm and 10 nm were e-beam evaporated on the GaN templates and then subjected to a thermal annealing process at 1000 $^\circ\text{C}$ for 60 minutes, for a fixed ratio of NH_3 to H_2 (1:3) gases inside the MOCVD chamber. GaN overgrowth was then made on these two templates at 1030 $^\circ\text{C}$, with constant TMGa flow rate of 78 $\mu\text{mol}/\text{min}$ and NH_3 flow rate of 7.6 l/min. For comparison, a control GaN layer was grown on the same GaN template using identical growth conditions but without the TiN network. The GaN sample with 20 nm TiN layer was characterized using cross-sectional and plane-view transmission electron microscopy (TEM), together with the control sample. Both samples were characterized by scanning electron microscope (SEM), x-ray diffraction (XRD), and room temperature time-resolved photoluminescence (TRPL). Table I summarized the growth conditions and characterization results for all the samples.

3 Results and Discussions SEM images show that the surface morphology of TiN covered template is strongly affected by annealing time, but to a lesser extent by different gas ratios and annealing temperatures. In the annealing process, microscopic windows were formed on the Ti layer due to desorption of the Ti layer at high temperatures, accompanied by nitridation of this discontinuous Ti layer into a TiN network. At the initial annealing stage, closed chains were formed on Ti film, with a feature size of $\sim 2 \mu\text{m}$. A similar phenomenon was reported by H. Mikaye et al [8]. We suggest that these small windows (chains) first appeared at grain boundaries of underlying GaN template at the initial stage of nitridation. The less impervious nature of GaN at the grain boundaries and a possible catalytic effect of Ti on GaN decomposition lead us to this suggestion. As the *in situ* annealing process progresses, new windows begin to form at the grain boundaries and consequently both the density and size of those win-

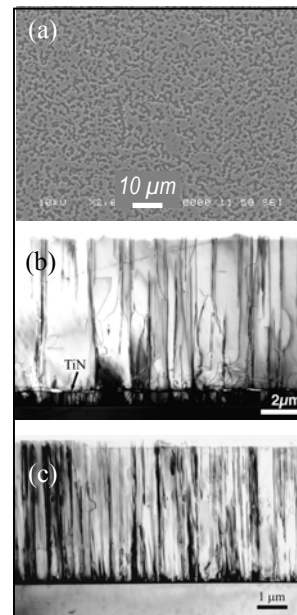


Fig. 1. (a) SEM of TiN porous network (20 nm Ti layer), formed by *in-situ* annealing in NH_3/H_2 (1:3). Cross sectional TEM showing the effect of TiN porous network (with 20 nm Ti layer) on GaN dislocation reduction (b), and (c) GaN layer control w/o TiN.

dows increase with time. Figure 1(a) shows the SEM surface morphology of TiN porous network formed on the 20 nm Ti layer.

The cross-sectional TEM micrograph for the GaN with the 20 nm TiN porous network is shown in Fig. 1(b). It can be seen that the GaN growth on the TiN porous network initiated from the microscopic windows of the discontinuous TiN network acting as GaN islands. This is followed by the growth of GaN emanating from the islands by lateral and vertical expansion leading to coalescence. It can be discerned that thin and flat surface voids are formed above the discontinuous TiN layer, due to the lateral overgrowth of GaN and the possible "antisurfactant effect" of TiN. Threading dislocations significantly decrease at or above the TiN/GaN interface. At least two mechanisms can be suggested for dislocation reduction related to GaN growth on TiN porous network. First, most of the threading dislocations in the GaN template are effectively blocked by the TiN layer. Second, some threading dislocations penetrate through the TiN windows to the upper layer but serendipitously change their propagation direction and extend laterally instead. In the near-dislocation-free region above TiN, some *c*-plane stacking faults are formed due to gliding and dissociation of dislocations into partials. Burger's vector permitting, additional dislocation reduction could occur through recombination and annihilation. Therefore, the propagation of dislocations is effectively suppressed near the TiN/GaN interface. For comparison, the control GaN layer grown without the TiN interlayer is shown in Fig. 1(c), which shows no observable dislocation reduction above the initial GaN template.

A precise assessment of the amount of dislocation reduction can be made by counting directly the dislocations in the plane-view TEM micrographs. In Fig. 2(a), the plane-view image of the GaN control layer grown without TiN (13 μm in thickness) shows a high density of edge dislocation arrays ($\sim 1.5 \times 10^9/\text{cm}^2$) as marked by "e", and a much lower density of isolated end-on screw dislocations ($\sim 1.3 \times 10^8/\text{cm}^2$) as marked by "s". For the GaN grown with 20 nm TiN porous network (thickness of only 7.5 μm) shown in Fig. 2(b), the screw dislocation density is almost unchanged ($\sim 1.4 \times 10^8/\text{cm}^2$), but the edge dislocations ($\sim 0.9 \times 10^8/\text{cm}^2$) have decreased by at least an order of magnitude. These plane-view images suggest that the thin TiN porous network used is very effective in reducing edge dislocations. For screw dislocations, their numbers are already low (about 10% of the total dislocations) in MOCVD GaN, and the effect of TiN in reducing them is therefore less likely.

High-resolution x-ray rocking curves (ω scan) show that the GaN samples grown on both 20 nm and 10 nm TiN porous networks have improved crystalline quality in terms of the full-width-at-half-maximum (FWHM) of the asymmetric (10 $\bar{1}2$) diffraction peaks, as can be seen in Table I. Specifically, for the GaN samples with 20 nm and 10 nm TiN porous networks, FWHMs of (10 $\bar{1}2$) peaks are 5.4

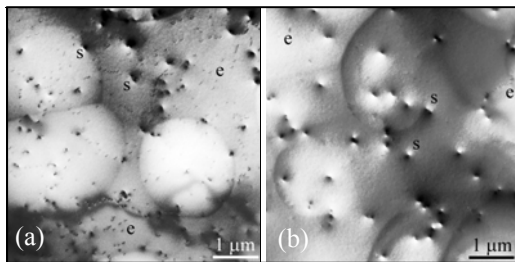


Fig. 2. Plane-view TEM micrographs showing the edge and screw dislocations at the top of GaN surface, for (a) the control sample without TiN, and (b) the GaN with 20 nm TiN porous network.

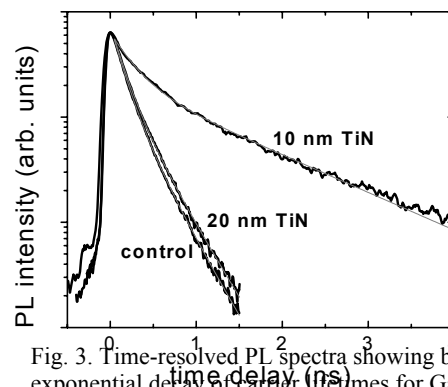


Fig. 3. Time-resolved PL spectra showing bi-exponential decay of carrier lifetimes for GaN grown on TiN porous networks using 20 nm and 10 nm Ti layer, and without TiN (control).

arcmin and 4.5 arcmin, respectively, as compared to 7.6 arcmin for the control sample. This is consistent

with the TEM results in Fig. 2, which showed $10 \times$ reduction in edge dislocations commonly associated with the asymmetric (10 $\bar{1}$ 2) broadening which is sensitive to edge dislocations. The nearly unaffected symmetric (0002) FWHM is consistent with the TEM micrographs showing unchanged screw dislocation density.

TRPL is a nondestructive and powerful technique commonly used to measure carrier lifetime, an important parameter related to material quality and device performance. Figure 3 shows the room temperature TRPL data for the GaN control sample (8 μm in thickness) with no TiN, and the GaN samples with 10 nm and 20 nm TiN porous networks. The time-resolved signals were integrated over a 10 nm-wide spectral region around the peak PL energy (3.40 eV). The instrument-limited rise implies that the relaxation processes to cool the carriers from 3.81 eV excitation energy-defined states to the zero momentum excitonic band edge states are very fast. For both samples, the decaying part of the TRPL data is well described by a bi-exponential decay function: $A_1 \exp(-t/\tau_1) + A_2 \exp(-t/\tau_2)$. Table I tabulates the decay constants (τ_1 and τ_2) and the amplitude ratios (A_2/A_1) obtained from the fits.

The fast decay constant τ_1 most probably represents the effective non-radiative recombination at room temperature. The slow decaying component τ_2 is attributed to the radiative lifetime of the free exciton. Compared to the control sample, GaN sample with 10 nm TiN porous network shows almost a factor of 2 improvement in the carrier lifetime (τ_2). The decay times for the GaN sample with 20 nm TiN network is similar to that for the control sample. However, the relative magnitude of the slow decaying component to the fast decaying component (A_2/A_1) for both of the samples with TiN networks are improved compared to the control sample. This indicates that the nonradiative recombination is reduced by the inclusion of the TiN porous network. The considerable increase in the carrier lifetime (τ_2) for the 10 nm TiN sample rather than the 20 nm sample is somewhat puzzling since the XRD data for both of these samples show similar characteristics. However, one should keep in mind that in addition to the threading dislocations, the carrier lifetime is also sensitive to other types of defects such as point defects, the effects of which are not manifested by XRD in these films with relatively broad X-ray diffraction peaks.

4 Conclusions In summary, we have demonstrated that the density of TDs can be reduced with an *in situ* TiN porous network. TEM images show that TiN is efficient in reducing threading dislocation density, particularly the edge type. XRD data indicate that the GaN films grown with a TiN network (both 20 nm and 10 nm Ti layer) have improved crystalline quality in terms of narrower asymmetric (10 $\bar{1}$ 2) peak FWHM, which substantiates the $10 \times$ reduction in edge dislocation density found by plane-view TEM, as compared to the GaN grown without a TiN layer. Time-resolved PL decay shows considerable increase in carrier lifetime with the use of TiN porous network, indicating reduced point defect density of the GaN epilayers.

Acknowledgements The work at VCU and Albany has been funded by ONR as part of a DURINT program and monitored by Dr. C. E. C. Wood of ONR. The authors have benefited from many helpful discussions with Prof. R. M. Feenstra. The authors also thank Prof. A. Baski and Prof. D. Johnstone for discussion. We acknowledge use of facilities in the John M. Cowley Center for High Resolution Electron Microscopy at Arizona State University.

References

- [1] H. Morkoç, "Nitride Semiconductors and Devices", Springer Verlag 1999, second editions in press.
- [2] M. A. Reshchikov and H. Morkoç, "Defects in GaN: Optical Signature", J. Appl. Phys. Reviews, under review.
- [3] See for example, P. Gibart, B. Beaumont, P. Vennéguès, "Epitaxial Lateral Overgrowth of GaN" in "Nitride Semiconductors, Chapter 2 in Handbook on Materials and Devices" Eds. P. Ruterana, M. Albrecht and J. Neugebauer, Eds. Wiley-VCH GmbH & Co.KgaA, Weinheim, ISBN: 3-527-40387-6 (2003).
- [4] S. Haffouz, B. Beaumont, P. vennegues, and P. Gibart, Phys. Status Solidi A **176**, 677 (1999).
- [5] S. Sakai, T. Wang, Y. Morishima, and Y. Naoi, J. Cryst. Growth **221**, 334 (2000).
- [6] Y. Oshima, T. Eri, M. Shibata, H. Sunakawa, and A. Usui, Phys. Stat. Sol. (a) **194**, No. 2, 554 (2002).
- [7] F. Yun, M. A. Reshchikov, K. Jones, P. Visconti, H. Morkoç, S. S. Park, and K. Y. Lee, Solid-State Elect. **44**, 2225 (2000).
- [8] H. Miyake, M. Yamaguchi, T. Maeda, and I. Akasaki, MRS Internet J. Nitride Semicond. Res. **551**, W2.3 (2000).